Atmospheric CH_3CCl_3 observations in China: Historical trends and implications

Dajiang Yu[1,2], Bo Yao[2,*], Weili Lin[3], Martin K. Vollmer[4], Baozhu Ge[5], Gen Zhang[6], Yi Li[6], Honghui Xu[7], Simon O'Doherty[8], Liqu Chen[2], Stefan Reimann[4]

[1] Longfengshan Regional Background Station, China Meteorological Administration (CMA), Heilongjiang, China

[2] Meteorological Observation Center (MOC) of China Meteorological Administration (CMA), Beijing, China

[3] College of Life and Environmental Sciences, Minzu University of China, Beijing, China

[4] Laboratory for Air Pollution and Environmental Technology (Empa), Swiss Federal Laboratories for Materials Science and Technology, Dübendorf, Switzerland

[5] State Key Laboratory of Atmospheric Boundary Layer Physics and Atmospheric Chemistry, Chinese Academy of Sciences, Institute of Atmospheric Physics, Beijing, China

[6] State Key Laboratory of Severe Weather & Key Laboratory of Atmospheric Chemistry of China Meteorological Administration (CMA), Chinese Academy of Meteorological Sciences (CAMS), Beijing, China

[7] Zhejiang Institute of Meteorological Sciences, Hangzhou, China

[8] Atmospheric Chemistry Research Group, University of Bristol, Bristol, UK

* Correspondence to: Bo Yao (yaob@cma.gov.cn)

Abstract

Although CH_3CCl_3 is an important ozone-depleting substance regulated by the Montreal Protocol on Substances that Deplete the Ozone Layer and its Amendments, the levels of atmospheric CH_3CCl_3 mixing ratios in China are poorly understood. Long-term *in-situ* measurements by GC-ECD have been conducted at the Shangdianzi Station in northern China since October 2006. In addition, air samples have been collected daily/weekly at seven stations and analyzed by GC/MS system since 2010. The two methods show comparable precisions at around 1% and all the measurements were calibrated by standards linked to the Advanced Global Atmospheric Gases Experiment (AGAGE) reference scale Scripps Institution of Oceanography (SIO)-05. Mixing ratios for both "background" and "polluted" conditions are reported. The atmospheric CH_3CCl_3 mixing ratios during background conditions showed a significant and consistent decreasing trend with a decline rate from 1.9 ppt/yr (October 2006 to December 2007) to 0.3 ppt/yr (November 2015 to December 2017) at the Shangdianzi Station. Measured background mixing ratios increased from 41% in 2007 to 95% in

2017. The mean mixing ratios and their enhancement of polluted conditions have decreased from 15.1 and 2.0 ppt in 2007 to 2.7 and 0.3 ppt in 2017 at Shangdianzi. The mixing ratios in air at background conditions at the seven stations in China agree well with each other and all decrease gradually. The percentage of pollution events to the total number of measurements (POL/SUM) at Lin'an has decreased significantly from 2010 to 2017, especially after 2013. In 2017, POL/SUMs of all stations were less than 8% and the enhancements above background were less than 0.7 ppt. Both mixing ratios and enhancements have decreased by one or two orders of magnitude when comparing the results from previous studies, in the early 2000s, with the results in 2017 from this study. Chinese emissions of CH_3CCl_3, which were estimated by a tracer-ratio method, have decreased from 1.6 kt/yr in 2007 to 0.3 kt/yr in 2013, indicating that CH_3CCl_3 has been phased-out in China in accordance with the Montreal Protocol.

Keywords: CH_3CCl_3, atmospheric mixing ratios, background levels, long-term trend, emissions

1 Introduction

CH_3CCl_3 (1,1,1,-trichloroethane or methyl chloroform) is a chlorinated compound that was widely used as an industrial solvent during the second half of the 20th century before it was recognized to be an ozone-depleting substance (ODS). CH_3CCl_3 use in metal and precision cleaning, and as solvent in adhesives and all the CH_3CCl_3 used eventually was emitted to the atmosphere (McCulloch and Midgley, 2001; Engel and Rigby, 2018). The primary atmospheric sink for CH_3CCl_3 is reaction with the hydroxyl radical (OH), providing an indirect method to determining global levels of the hydroxyl radical (OH) (Prinn et al., 2005). A significant fraction of emitted CH_3CCl_3 enters the stratosphere due to its relatively long lifetime, where it is photolyzed, releasing chlorine atoms which catalytically destroy ozone.

Because CH_3CCl_3 contributes significantly to ozone depletion (Montzka and Reimann, 2011), it was recognized as a first generation ODS and restricted by the London Amendment of the Montreal Protocol in the 1990s. The production and consumption of CH_3CCl_3 were phased-out in developed countries by 1996, but were still allowed in developing countries in decreasing amounts until 2015 (UNEP, 2003). Based upon government and industry reports, consumption of CH_3CCl_3 in the U.S. is estimated to have fallen to zero in 1997 (McCulloch and Midgley, 2001). The estimated European emissions, based on atmospheric measurements, decreased dramatically from 60 kt/yr in the 1990s to 0.3~3.4 kt/yr in 2000~2003 (Reimann et al., 2005) and 0.3 kt/yr in 2012 (Maione et al., 2014). As the lifetime of CH_3CCl_3 is only 5 years (WMO, 2018), significant decreasing trends of global atmospheric CH_3CCl_3 concentrations were reported in the 2010, 2014, and 2018 Scientific Assessment of Ozone Depletion of the World Meteorological Organization (WMO) (Montzka and Reimann, 2011; Carpenter and Reimann, 2014; Engel and Rigby, 2018). However, recent studies revealed unexpected emissions of several first generation ODSs including CH_3CCl_3, CFC-11, and CCl_4 at a global scale (Montzka et al., 2018) or from

a specific region (Maione et al., 2014; Lunt et al., 2018; Rigby et al., 2019), nearly a decade after they were totally banned. Therefore, it is important to conduct long-term measurements of ODSs including CH_3CCl_3 to track their atmospheric trends, which can help evaluating the effectiveness of the phase-out policies.

China is one of the most populated and fastest developing countries classified under the Montreal Protocol as an "Article 5 country''. Under the Montreal Protocol, China was required to achieve a 30% reduction from the base level (average of 1998 to 2000 production and consumption) by 2005, a 70% reduction by 2010 and a 100% reduction by 2015 with possible essential use exemptions (UNEP, 2003). With the support from the Multilateral Fund for Implementation of the Montreal Protocol, China has implemented a strategy to accelerate the phase-out of primary ODSs, including CH_3CCl_3, resulting in a total ban of CH_3CCl_3 in 2010, 5 years ahead of schedule. In the last two decades, several studies on Chinese CH_3CCl_3 measurements were conducted during campaigns mainly focusing on cities or industrialized areas, especially in Southern China (Barletta et al., 2006; Chan et al., 2006; Chang et al., 2008; Shao et al., 2011). However, studies based on long-term observations or in multiple regions in China have not been reported. Few results since 2010 were available when CH_3CCl_3 was totally banned (Zheng et al., 2019), thus a comprehensive study of atmospheric CH_3CCl_3 observation in China is urgently needed.

In this study, long-term *in-situ* measurements of CH_3CCl_3 at a background station in northern China since 2006 and daily/weekly sampling analysis at seven stations since 2010 were conducted. We report mixing ratios for both "background" and "polluted" conditions. Background trends are analyzed and compared with global trends, while characteristics of polluted conditions among different stations are presented and discussed. Additionally, Chinese CH_3CCl_3 emissions from 2007 to 2013 are estimated by a tracer-ratio method, using carbon monoxide (CO) as a tracer.

2 Method

2.1 Site description

The locations of the seven background stations in this study are shown in Fig. 1 and their geographic information, measurement details and representativeness are listed in Table S1. All of these stations are operated by the China Meteorological Administration (CMA). Among them, Mt. Waliguan (WLG) and Shangri-La (XGL) are high-altitude stations with elevations larger than 3500 m, representing background conditions. The other five stations (Shangdianzi (SDZ), Lin'an (LAN), Heyuan (HYN), Jiangjin (JGJ) and Longfengshan (LFS)) are located in rural areas near or downwind of the most important populated and industrial regions in China, e.g. the Northern China Plain, the Yangtze River Delta, the Pearl River Delta, the Sichuan Basin as well as the Northeast China Plain, respectively.

All the stations are at least 20 km away from densely populated or industrialized cities. The sample inlets are mounted at the top of towers (80 meters for WLG, SDZ,

LFS, 50 meters for LAN, XGL and 10 meters for HYN, JGJ) at all stations to avoid local contamination and ensure regional representativeness.

2.2 *In-situ* measurements at the Shangdianzi Station

Air samples were analyzed *in-situ* at SDZ by a gas chromatographic (GC, Agilent 6890N, USA) system with two electron capture detectors (ECD) equipped with a custom-built sample preparation system (SPS). The system was installed in October 2006 and the technical details were reported by Vollmer et al. (2009) and Yao et al. (2012a).

Air samples were taken from the top of a tower and were continuously drawn through a 10 mm O.D. tubing (Synflex-1300, USA) by means of a membrane pump (KNF-86, KNF Neuberger, Germany), resulting in a response time of < 5 min. Each air sample was bracketed by a reference sample (working standard or quaternary standard) to detect and correct for drift in the detector sensitivity for each air sample. Air samples were analyzed every 80 minutes. The CH_3CCl_3 measurements were linked to the Advanced Global Atmospheric Gases Experiment (AGAGE) (Prinn et al., 2000; Prinn et al., 2018) and reported as dry air mole fractions on the Scripps Institution of Oceanography SIO-05 calibration scale. CO has also been measured *in-situ* at SDZ since February 2007 by a non-dispersive infrared (NDIR) method (Horiba AMPA-360CE) with a time resolution of 1 min. The system shared the same inlet with the GC-ECD system and the measurement precision is <10 ppb. The CO data are reported on World Meteorological Organization (WMO)-2014A calibration scale and used to estimate CH_3CCl_3 emission by a tracer-ratio method, which is discussed in section 2.4.

2.3 Canister sampling

At all seven stations, air samples were collected in 3-L stainless steel canisters (X23-2N, LabCommerce, Inc, USA) by custom made samplers. Air was drawn into the canisters by means of a membrane pump (KNF-86, KNF Neuberger, Germany). The canisters were flushed by ambient air for 10 min with a constant flow rate of 2 L min, and then it was pressurized to 20 psi above ambient pressure (Zhang et al., 2017). The recoveries for CH_3CCl_3 were 99% to 101% after air from standards were sampled and stored in the canisters for 9 to 112 days.

Ambient air was drawn from the top of the sampling towers at each station. At WLG, SDZ, LAN, LFS and XGL, a pair of samples was collected in series every week since 2010, while daily air samples were collected without duplicates at HYN and JGJ since 2017.

To minimize the effects of local pollution and ensure the regional representativeness, samples were collected at 08:00 (local time) at WLG, because of the unique landform of this high-altitude station (Zhou et al., 2003). At other sites, samples were collected at 14:00 (local time), when the height of local mixed layer reached maximum to possibly minimize the affection of local pollution (Miao et al., 2015, 2017). When the wind speed was lower than 2 m/s or there were other deleterious weather conditions such as fog, rain or haze, sampling was delayed.

A sample preparation unit (Medusa) with GC and mass spectrometric detection (MS) (Miller et al., 2008) was used to analyze the air samples in the greenhouse lab of the Meteorological Observation Center (MOC) of CMA within one month. The same calibration procedure as for the GC-ECD system was followed and the measurements were also linked to the SIO-05 calibration scale for CH_3CCl_3. The details of the sampling, analysis and calibration were described by Zhang et al. (2017).

2.4 Emission estimation by tracer-ratio method

The tracer-ratio method was used to estimate Chinese ODS emissions in previous studies (Li et al., 2011; Palmer et al., 2003; Shao et al. 2011; Fang et al., 2012; Yao et al., 2012b). The method is based on the assumption that the target ODS and the chosen tracer are either emitted from the same source or are well mixed during transport to the measurement site, thus the ratio of their mixing ratio enhancements remains constant during the transport from the source to the observed site.

CO is a commonly chosen tracer (Palmer et al., 2003; Shao et al. 2011; Fang et al., 2012; Yao et al., 2012b) because both CO and ODSs emissions are mainly of anthropogenic origin and the CO emissions from China are relatively well known (Ohara et al., 2007; Streets et al., 2003; Zhang et al., 2009). In this study, the correlation coefficient between CH_3CCl_3 and CO was statistically significant ($p<0.01$) from the *in-situ* measurements at Shangdianzi during 2007 to 2013, showing Pearson correlation coefficients larger than 0.2. The correlation was not significant for the *in-situ* measurement at Shangdianzi from 2014 to 2017, neither for the sampling measurement at all the seven stations from 2011 to 2017, mainly due to very limited pollution events.

The details of the tracer-ratio method have been described in a previous study by Yao et al (2012b). Here we briefly introduce the method. Emissions of CH_3CCl_3 (E_{MC}) can be calculated from its mixing ratio enhancement (mixing ratio during pollution events minus that during baseline conditions, ΔC_{MC}) and the mixing ratio enhancement of CO (ΔCO) by:

$$E_{MC} = E_{CO} b \frac{M_{MC}}{M_{CO}}, \text{ with } b = \frac{\Delta C_{MC}}{\Delta C_{CO}} \qquad \text{Eq. 1.}$$

Here E_{co} represent CO emissions, M_{MC} and M_{CO} are the molecular weights of CH_3CCl_3 and CO, respectively. The uncertainty of the CH_3CCl_3 emission estimate (σ_{MC}) is given by error propagation

$$\sigma_{MC} = E_{MC} \sqrt{\left(\frac{\sigma_b}{b}\right)^2 + \left(\frac{\sigma_{E_{CO}}}{E_{CO}}\right)^2} \qquad \text{Eq. 2.}$$

Here, σ_b and $\sigma_{E_{CO}}$ represent the uncertainty of the tracer ratio *b* and the CO emissions.

The measurements at SDZ are sensitive to emissions from provinces in the Northern China Plain as well as the Yangtze River Delta, including the Chinese provinces of Anhui, Beijing, Hebei, Henan, Jiangsu, Jilin, Liaoning, Inner Mongolia, Shandong,

Shanxi, and Tianjin, but other parts of China are not sampled (Yao et al., 2012b). So we first estimate the emissions for the provinces mentioned above (called North China Plain afterwards, or in abbreviation as NCP) and then extrapolated to the emission of the whole China, assuming that the ratio of enhanced CH_3CCl_3 mixing ratios to enhanced CO mixing ratios is the same for the rest of the country.

The tracer ratio *b* and its uncertainty are estimated using the weighted total least square (WTLS) regression of a straight line with uncertainties in both coordinates (Krystek and Anton, 2007). Total Chinese CO emissions from 2007 to 2013 were calculated using CO emissions of 166.9 Mt/yr for 2006 and a growth rate of 3.4%/yr (Zhang et al. 2009), assuming that the growth rate for 2007 to 2013 remains the same as the rate for 2001 to 2006. The uncertainty of Chinese CO emissions during 2007 to 2013 is estimated as ±37.8% by combining the uncertainty of the Chinese CO emissions in 2006 (±35%) reported by Zhang et al. (2009) and an estimated uncertainty of the growth rate of ±100%. CO emissions from the NCP are 88 Mt/yr in 2006 (Zhang et al., 2009) and we assumed the same growth rate as the whole country. An additional uncertainty of 10% is used to account for representativeness uncertainties when NCP emission extrapolated to total Chinese emissions.

3 Results and discussion

3.1 Comparison between *in-situ* and weekly sampling measurements

Both *in-situ* measurement by the GC-ECD system and the canister sampling measurements were conducted at the SDZ station. The precision of the *in-situ* measurements for the GC-ECD is estimated by the standard deviation of a measured target tank (working standards analyzed with the same procedure as ambient samples) (Yao et al., 2014). The precision of the GC-ECD system was 0.7%, this was determined by analyzing the target tanks 57 times. Furthermore, the air from the target tank was filled into canisters and analyzed by GC/MS with the same procedure as for ambient samples, then the precision of sampling method were calculated as 1.1% by analyzing 16 target canister samples. Thus, the precision of the two methods are comparable.

The results of co-located *in-situ* measurements and canister sampling at SDZ from 2010 to 2015 were compared by using the *in-situ* air measurements closest in time to when the weekly canister samples were taken. As shown in Fig. S1, the differences between the mixing ratios of the two methods in the same time window were all centered within at -0.4 to 0.4 ppt, and 80% of the differences were from -0.2 to 0.2 ppt. The difference between the concentrations of the two methods are most likely caused by sampling time synchronization of two systems. Overall, this suggests that the two methods agreed well.

3.2 Time series and background trends of *in-situ* measurement at the Shangdianzi Station

Fig. S2 shows time series of the CH_3CCl_3 mixing ratios of the *in-situ* measurements by the GC-ECD system at SDZ from October 2006 to December 2017.

We used a robust local regression mathematic procedure to distinguish mixing ratio in background and polluted conditions (Ruckstuhl et al., 2012). The filter fits a local regression curve to the data using robustness weights for values above the baseline and iteratively excluding data points outside a 1-sigma range around the current baseline. Yearly average mixing ratios and their standard deviation (1-sigma) are calculated for *in-situ* CH_3CCl_3 measurements for each year. The yearly mean values, standard deviation and the percentage of background conditions are list in Table 1, together with the percentile of the mixing ratios representing pollution events.

The percentage of background values for CH_3CCl_3 increased from 41% in 2007 to 95% in 2017, suggesting that fewer pollution events were observed at SDZ from year to year. As shown in Fig. 2, the long-term trends are estimated based on linear curve fitting of the CH_3CCl_3 background mixing ratios. The rate of decline for CH_3CCl_3 at SDZ become smaller over time. From October 2006 to December 2007, the decline is -1.9 ppt/yr, consistent with global trend from 2007 to 2008 by the *in-situ* network of NOAA (-1.9 ppt/yr) and AGAGE (-2.0 ppt/yr) (Montzka and Reimann, 2011). Then the rate of decline decreased to -1.3 ppt/yr from January 2008 to December 2012, agree well with the trend determined from 2011 to 2012 by the AGAGE and NOAA networks (both were -1.06 ppt/yr) (Carpenter and Reimann, 2014). From March 2013 to November 2014, November 2015 to December 2017, the trends were -0.8ppt/yr and -0.3ppt/yr, respectively, in accordance with the trend of -0.48 ppt/yr from 2015 to 2016 by AGAGE (Engel and Rigby, 2018).

Elevated CH_3CCl_3 mixing ratios at SDZ were observed frequently until 2011, mainly due to polluted air masses transported from urban or industrialized areas. However, after the production and consumption were totally banned at the end of 2010, the enhancements dropped dramatically from up to several tens of ppt occurred every year from 2006 to 2010 to the low ppt level since 2011, or even less than 1 ppt since 2013. This indicates the success of the Montreal Protocol in substantially decreasing CH_3CCl_3 production and consumption in China. A similar trend was observed from the European background stations (e.g. Mace Head (MHD), Ireland), after the production and consumption of CH_3CCl_3 was banned in non-Article 5 (developed) counties.

3.3 Comparison of mixing ratios of 7 Chinese background stations

Time series of CH_3CCl_3 at 7 Chinese stations from 2010 to 2017 are shown in Fig. S3. Both background signals and occasional pollution events were captured. Regional background and pollution conditions of the results were distinguished by combing a statistical filter using a “robust local regression” mathematical procedure (Ruckstuhl et al., 2012) and a background wind sector method (Zhou et al., 2003). The background wind sectors were defined by the local pollution sources and the characteristics of other tracers such as CO and HCFCs (Yao et al., 2012a; Zhang et al., 2017).

The trends of CH_3CCl_3 background mixing ratios at the seven stations show similar patterns and were consistent with *in-situ* data at SDZ. Fig. 3 shows the annual statistical result (mean, median, 5-, 25-, 75- and 95 percentiles) of CH_3CCl_3 at each of the seven stations from 2011 to 2017, compared with yearly mean background mixing ratios of

MHD which represent the global background of northern hemisphere. It should be noted that the observation at XGL started in June 2011 and the HYN and JGJ station only have 2017 data. No significant differences are observed among all the stations from year to year. The background mixing ratios of CH_3CCl_3 at five sites with longer observation periods agreed well with MHD and show similar decreasing trends even though they present background conditions for different regions, e.g. the Qinghai-Tibet Plateau and populated areas such as the North China Plain or the Yangtze River Delta.

Very infrequent pollution events were exhibited at the remote stations, WGL and XGL, two events and one event respectively. The number and mean mixing ratio of polluted samples at the other 5 stations in this study are shown in Table 2. For SDZ and LFS, less than 5 samples were selected as polluted every year. At LAN, the percentage of pollution events has decreased significantly from 2010 to 2017, especially after 2013.The yearly averaged enhancements at LAN in all years were lower than 1 ppt with the exception of 2016 when only two samples were selected as polluted. In 2017, The percentages of pollution events to the total number of measurements (POL/SUMs) of all 5 stations (LAN, SDZ, LFS, JGJ, HYN) were less than 8% and the enhancements are all less than 0.7 ppt, revealing only individual pollution events with low enhancement were observed.

3.4 Comparison of CH_3CCl_3 results with previous studies in China

To evaluate the effectiveness of the CH_3CCl_3 phase-out policies implemented in China, it is crucial to characterize the spatial and temporal variations of CH_3CCl_3 mixing ratios in polluted air masses in China before and after production and consumption of CH_3CCl_3 were regulated. In this study, we compare mixing ratios of CH_3CCl_3 at LAN, LFS, SDZ, HYN and JGJ with other results by previous studies in populated areas or in background stations but for polluted events in China.

As shown in Fig. 4, the atmospheric mixing ratios of CH_3CCl_3 in the Pearl River Delta have exhibited dramatically decreasing trends over the last 17 years, this is one of the most developed regions in China and a potential emission source of CH_3CCl_3. Before CH_3CCl_3 was regulated in China, its mixing ratios reached 60 to 93 ppt in the Pearl River Delta in 2000 and 2001 (Chan et al., 2006; Chan et al., 2007), which were approximately 20 to 50 ppt higher than the global background level at that time. The mixing ratio of CH_3CCl_3 dropped to 52 ppt in 2004 in Guangzhou city (Chang et al., 2008; Shao et al., 2011), approximately 30 ppt higher than global background level, while the observation at rural sites in the Pearl River Delta and in Taiwan in 2004 and 2005 varied from 33 to 70 ppt (Lee et al., 2007; Chang et al., 2008; Shao et al., 2011), indicating large on-going CH_3CCl_3 emission in this region. In 2007, when Chinese CH_3CCl_3 production and consumption was reduced by 30%, CH_3CCl_3 mixing ratios were reported at 32 and 53 ppt at two rural sites in the Pearl River Delta (Zhang et al., 2010), approximately 146% and 300% higher than global background levels. However, only few pollution events were captured by daily sampling at Heyuan, a background station in the Pearl River Delta in 2017 by this study, and the averaged mixing ratio was 2.4 ppt, less than 10% higher than background mixing ratios. Due to limited

observations were conducted from 2008 to 2016 in the Pearl River Delta, it is difficult to trace back the details how the CH_3CCl_3 mixing ratio changed in the last 10 years. In conclusion, both mixing ratios and enhancements have decreased by one or two orders of magnitude, by comparing the results from 2000 to 2007 by previous studies with the results of 2017 by this study in the Pearl River Delta, which indicates CH_3CCl_3 has been phased down well in southern China. It should be noted that the studies discussed here were linked to different calibration scales, e.g. SIO, UCI or TO-14A scales. However, the differences between the calibration scales are only few per cent for CH_3CCl_3 (Hall et al., 2014), much smaller than the differences between studies in early 2000s or the range of decreasing trend from early 2000s to 2017.

Similar trends were found in other cities or regions in China. The averaged mixing ratio of 45 cities by Barletta et al. (2006) was at 49 ppt in 2001, approximately tens of ppt higher than global background level. The CH_3CCl_3 mixing ratios observed at rural sites and oil field at the Yellow River Delta in 2017 is only 0.2 to 0.4 ppt higher than the background level of SDZ (Zheng et al., 2019), and agree well with averaged enhancement of pollution event at SDZ (0.3 ppt) in 2017, revealing no strong pollution events in the North China Plain observed in recent years.

3.5 Emission estimated by the tracer-ratio method

The regression analysis of enhanced CH_3CCl_3 mixing ratio versus enhanced CO mixing ratios during 2007 to 2013 is shown in Fig. S4 and the CH_3CCl_3 emissions from the NCP and the whole China are listed in Table 3.

CH_3CCl_3 emissions for both the NCP and whole China show a continuous decline from 2007 to 2013. The total Chinese emissions have decreased from 1.6 kt/yr (2007) to 0.3 kt/yr (2013), indicating the effectiveness of the Montreal Protocol in substantially decreasing CH_3CCl_3 emissions. The estimated CH_3CCl_3 emissions of the years 2007 and 2008 for the whole China were 1.6 and 1.5 kt/yr, respectively, which agree quite well with Chinese emission of 1.7 kt/yr for the period from December 2007 to December 2008 based on the *in-situ* measurement at the Gosan Station, Korea (Li et al, 2011), and were much smaller than 10.4 kt/yr for the year 2001 based on aircraft measurements downwind of China (Palmer et al., 2003). Cumulative Chinese emissions from 2007 to 2013 (6.2 kt) accounted for approximately 21% of the global emissions (29 kt) during the same time period (Engel and Rigby, 2018).

4 Conclusions

Atmospheric CH_3CCl_3 mixing ratios were obtained in China by high-frequency, *in-situ* measurements at the Shangdianzi Station with a GC-ECD system from 2006 to 2017, as well as weekly sampling at 5 stations from 2010 to 2017 and daily sampling at 2 stations in 2017. Results from the co-located *in-situ* measurement and weekly taken samples at SDZ agree well with each other. The background mixing ratios of the 7 stations show similar trends and are consistent with global background level. Few pollution events were observed at the remote stations WLG and XGL, whilst the percentage of background conditions at LAN increased strongly, especially since 2013.

In 2017, only individual pollution events were observed with rather low enhancement. Both the mixing ratios and the enhancements have decreased by one or two orders of magnitude, compared to the result reported in previous studies in the Pearl River Delta at the beginning of this century. The Chinese CH_3CCl_3 emissions estimated by the tracer-ratio method shows a continuously decline trend from 2007 to 2013, revealing the effectiveness of phasing out CH_3CCl_3 in China.

Acknowledgments

This work is supported by the National Nature Science Foundation of China (41575114 & 41730103). The stations personnel have supported the *in-situ* measurements and weekly canister sampling at SDZ, WLG, LAN, LFS, XGL, JGJ and HYN. This work has benefited from technical assistance by the AGAGE (System for Medusa-GC/MS) and the SOGE (System for GC-ECD) networks. The Scripps Institution of Oceanography (SIO) is acknowledged for help with the data acquisition and processing software and providing calibration standards. The operation of the Mace Head station is funded by the UK Department of Business, Energy and Industrial Strategy (BEIS) through contract TRN 1537/06/2018 with additional funding at Mace Head under NASA contract NNX16AC98G through MIT. We also thank Matthew Rigby from the University of Bristol for providing global CH_3CCl_3 emissions estimates.

References

Barletta, B., Meinardi, S., Simpson, I., Rowland, F.S., Chan, C., Wang, X., Zou, S., Chan, L., Blake, D.R., 2006. Ambient halocarbon concentrations in 45 Chinese cities. Atmos. Environ. 40, 7706–7719.

Chan, C.Y., Tang, J.H., Li, Y.S., Chan, L.Y., 2006. Mixing ratios and sources of halocarbons in urban, semi-urban and rural sites of the Pearl River Delta, South China. Atmos. Environ. 40, 7331-7345.

Chan, L.Y and Chu, K.W, 2007. Halocarbon in the atmosphere of the industrial-related Pearl River Delta region of China. J. Geophys. Res. 112, D04305.

Chang, C.-C., Lai, C.-H., Wang, C.-H. Liu, Y., Shao, M., Zhang, Y., Wang, J.-L., 2008. Variability of ozone depleting substances as an indication of emissions in the Pearl River Delta, China. Atmos. Environ. 42, 6973–6981.

Carpenter, L.J. and Reimann, S., 2014. Ozone-Depleting Substances (ODSs) and Other Gases of Interest to the Montreal Protocol, Chapter 1 in Scientific Assessment of Ozone Depletion: 2014, Global Ozone Research and Monitoring Project – Report No. 55, World Meteorological Organization, Geneva, Switzerland.

Engel, A. and Rigby, M., 2018. Update on Ozone-Depleting Substances (ODSs) and Other Gases of Interest to the Montreal Protocol, Chapter 1 in Scientific Assessment of Ozone Depletion: 2018, Global Ozone Research and Monitoring Project–Report No. 58, World Meteorological Organization, Geneva, Switzerland.

Fang, X., Wu, J., Su, S., Han, J., Wu, Y., Shi, Y., Wan, D., Sun, X., Zhang, J., Hu. J., 2012. Estimates of major anthropogenic halocarbon emissions from China based on interspecies correlations. Atmos. Environ. 62, 26-33.

Hall, B.D., Engel, A., Mühle, J., Elkins, J.W., Artuso, F., Atlas, E., Aydin, M., Blake, D., Brunke, E.-G., Chiavarini, S., Fraser, P. J., Happell, J., Krummel, P.B., Levin, I., Loewenstein, M., Maione, M., Montzka, S.A., O'Doherty, S., Reimann, S., Rhoderick, G., Saltzman, E.S., Scheel, H.E., Steele, L.P., Vollmer, M.K., Weiss, R.F., Worthy, D., Yokouchi, Y., 2014. Results from the International Halocarbons in Air Comparison Experiment (IHALACE). Atmos. Meas. Tech., 7, 469–490.

Lee, B.-S., Chiou, C.-B.,2007. The Use of CFC-12, CFC-11 and CH_3CCl_3 to trace terrestrial airborne pollutant transport by land-Sea breezes. Atmos. Environ. 41, 3360–3372.

Li, S., Kim, J., Kim, K. R., Mühle, J., Kim, S. K., Park, M.K., Stohl, A., Kang, D.J., Arnold, T., Harth, C.M., Salameh, P.K., Weiss, R.F., 2011. Emissions of halogenated compounds in East Asia determined from measurements at Jeju Island, Korea. Environ. Sci. Technol. 45, 5668-5675.

Lunt, M.F., Park, S., Li, S., Henne, S., Manning, A.J., Ganesan, A.L., Simpson , I.J., Blake, D.R., Liang, Q., O'Doherty, S., Harth, C.M., Mühle, J., Salameh, P.K., Weiss, R.F., Krummel, P.B., Fraser, P.J., Prinn, R.G., Reimann, S. , Rigby, M., 2018. Continued emissions of the ozone-depleting substance carbon tetrachloride from eastern Asia. Geophys Res Lett 45, 11423-11430.

Miao, Y.C., Hu, X.M., Liu, S.H., Qian, T.T., Xue, M., Zheng, Y.J., Wang, S., 2015. Seasonal variation of local atmospheric circulations and boundary layer structure in the Beijing-Tianjin-Hebei region and implications for air quality. J. Adv. Model. Earth Syst. 7, 1602-1626.

Miao, Y.C., Guo, J.P., Liu, S.H., Liu, H., Li, Z.Q., Zhang, W.C., Zhai, P.M., 2017. Classification of summertime synoptic patterns in Beijing and their associations with boundary layer structure affecting aerosol pollution. Atmos. Chem. Phys. 17, 3097-3110.

Miller, B.R., Weiss, R.F., Salameh, P.K., Tanhua, T., Greally, B.R., Mühle, J., Simmonds, P.G., 2008. Medusa: A sample preconcentration and GC/MS detector system for in situ measurements of atmospheric trace halocarbons, hydrocarbons, and sulfur com- pounds. Anal. Chem. 80, 1536–1545.

McCulloch, A. and Midgley, P.M., 2001. The history of methyl chloroform emissions: 1951–2000. Atmos. Environ. 35, 5311–5319.

Maione, M., Graziosi, F., Arduini, J., Furlani, F., Giostra, U., Blake, D.R., Bonasoni, P., Fang, X., Montzka, S.A., O'Doherty, S.J., Reimann, S., Stohl, A., Vollmer, M.K., 2014. Estimates of European emissions of methyl chloroform using a Bayesian inversion method. Atmos. Chem. Phys. 14, 9755-9770.

Montzka, S.A. and Reimann, S., 2011. Ozone-depleting substances (ODSs) and related chemicals. In Scientific Assessment in Ozone Depletion: 2010, Chapter 1, Global Ozone Research and Monitoring Project-Report No. 52, World Meteorological Organization: Geneva, Switzerland.

Montzka, S.A., Dutton, G.S., Yu, P., Ray, E., Portmag. W., Daniel, J.S., Kuijpers, L., Hall, B.D., Mondeel, D., Siso, C., Nance, J.D., Rigby, M., Manning, A. J., Hu, L. J, Moore, F., Miller, B.R., Elkins J.W., 2018. An unexpected and persistent increase in global emissions of ozone-depleting CFC-11. Nature 557, 413-417.

Krystek, M. and Anton, M., 2007. A weighted total least-squares algorithm for fitting a straight line. Meas. Sci. Tech. 18, 3438–3442.

Ohara, T., Akimoto, H., Kurokawa, J., Horii, N., Yamaji, K., Yan, X., Hayasaka, T., 2007. An Asian emission inventory of anthropogenic emission sources for the period 1980–2020. Atmos. Chem. Phys. 7, 4419–4444.

Palmer, P.I., Jacob, D.J., Mickley, L.J., Blake, D.R., Sachse, G.W., Fuelberg, H.E., Kiley, C.M., 2003. Eastern Asian emissions of anthropogenic halocarbons deduced from aircraft concentration data. J. Geophys. Res. 108(D24), 4753.

Prinn, R.G., J. Huang, R. Weiss, D. Cunnold, P. Fraser, P. Simmonds, A. McCulloch, C. Harth, S. Reimann, P. Salameh, S. O'Doherty, R.H.J. Wang, L. Porter, B.R. Miller, Krummel, P., 2005. Evidence for variability of atmospheric hydroxyl radicals over the past quarter century. Geophys. Res. Lett. 32, L07809.

Prinn, R.G., Weiss, R.F., Arduini, J., Arnold, T., DeWitt, H.L., Fraser, P.J., Ganesan, A.L., Gasore, J. Harth, C.M., Hermansen, O., Kim, J., Krummel, P.B., Li, S., Loh, Z.M., Lunder, C.R., Maione, M., Manning, A.J., Miller, B.R., Mitrevski, B., Mühle, J., O'Doherty, S., Park, S., Reimann, S., Rigby, M., Saito, T., Salameh, P.K., Schmidt, R., Simmonds, P.G., Steele, L.P., Vollmer, M.K., Wang, R.H., Yao, B., Yokouchi, Y., Young, D., Zhou, L., 2018. History of chemically and radiatively important atmospheric gases from the Advanced Global Atmospheric Gases Experiment (AGAGE). Earth Syst. Sci. Data 10, 985–1018.

Prinn, R.G., Weiss, R.F., Fraser, P.J., Simmonds, P.G., Cunnold, D.M., Alyea, F.N., O'Doherty, S., Salameh, P., Miller, B.R., Huang, J., Wang, R.H.J., Hartley, D.E., Harth, C., Steele, P., Sturrock, G., Midgley, P.M., McCulloch, A., 2000. A history of chemically and radiatively important gases in air deduced from ALE/GAGE/AGAGE. J. Geophys. Res. 105, 17751– 17792.

Reimann, S., Manning, A. J., Simmonds, P. G., Cunnold, D. M., Wang, R. H. J., Li, J., McCulloch A., Prinn, R. G., Huang, J., Weiss, R. F., Fraser, P. J., O'Doherty, S., Greally, B. R., Stemmler, K., Hill, M., Folini, D., 2005. Low European methyl chloroform emissions inferred from long-term atmospheric measurements. Nature 433, 506–508.

Rigby, M., Park, S., Saito, T., Western, L.M., Redington, A.L., Fang, X., Henne, S., Manning, A.J., Prinn, R.G., Dutton, G.S., Fraser, P.J., Ganesan, A.L., Hall, B.D., Harth, C.M., Kim, J., Kim, K.R., Krummel, P.B., Lee, T., Li, S., Liang, Q., Lunt, M.F., Montzka, S.A., Mühle, J., O'Doherty, S., Park, M.K., Reimann, S., Salameh, P.K., Simmonds, P., Tunnicliffe, R.L., Weiss, R.F., Yokouchi, Y., Young, D., 2019. Increase in CFC-11 emissions from eastern China based on atmospheric observations. Nature, 569(7757),546-550.

Rigby, M., Prinn, R.G., O'Doherty, S., Miller, B.R., Ivy, D., Mühle, J., Harth, C.M., Salameh, P.K., Arnold, T., Weiss, R.F., Krummel, P.B., Steele, L.P., Fraser, P.J., Young, D., Simmonds, P.G., 2014. Recent and future trends in synthetic greenhouse gas radiative forcing. Geophys. Res. Lett. 41(7), 2623−2630.

Ruckstuhl, A.F., Henne, S., Reimann, S., Steinbacher, M., Buchmann, B., Hueglin, C., 2012. Extraction of baseline signal of atmospheric trace species using local regression. Atmos. Meas. Tech. 5, 2613-2624.

Shao, M., Huang, D., Gu, D., Lu, S., Chang, C., Wang J., 2011. Estimate of anthropogenic halocarbon emission based on measured ratio relative to CO in the Pearl River Delta region, China. Atmos. Chem. Phys. 11, 5011–5025.

Streets, D.G., Bond, T.C., Carmichael, G.R., Fernandes, S.D., Fu, Q., He, D., Klimont, Z., Nelson, S.M., Tsai, N.Y., Wang, M.Q., Woo, J.-H., Yarber, K.F., 2003. An inventory of gaseous and primary aerosol emissions in Asia in the year 2000. J. Geophys. Res. 108, 8809.

UNEP (United Nations Environment Programme), 2003. Handbook for the international treaties for the protection of the ozone layer (Sixth edition). Nairobi, Kenya.

Vollmer, M.K., Zhou, L.X., Greally, B.R. Henne, S., Yao, B., Reimann, S., Stordal, F., Cunnold, D.M., Zhang, X.C., Maione, M., Zhang, F., Huang, J., Simmonds, P.G., 2009. Emissions of ozone-depleting halocarbons from China. Geophys. Res. Lett. 36, L15823.

WMO (World Meteorological Organization), 2018. Scientific Assessment of Ozone Depletion: 2018, Global Ozone Research and Monitoring Project–Report No. 58, Geneva, Switzerland.

Yao, B., Vollmer, M.K., Xia, L., Zhou, L., Simmonds, P.G., Stordal, F., Maione, M., Reimann, S., O'Doherty, S., 2012a. A study of four-year HCFC-22 and HCFC-142b in-situ measurements at the Shangdianzi regional background station in China. Atmos. Environ. 63, 43-49.

Yao, B., Vollmer, M.K., Zhou, L.X., Henne, S., Reimann, S., Li, P.C., Wenger, A., Hill, M., 2012b. In-situ measurements of atmospheric hydrofluorocarbons (HFCs) and perfluorocarbons (PFCs) at the Shangdianzi regional background station, China. Atmos. Chem. Phys. 12, 10181-10193.

Yao, B., Zhou, L., Xia, L., Zhang, G., Guo, L., Zhao, L., Fang, S., 2014. Atmospheric sulfur hexafluoride in-situ measurements at the Shangdianzi regional background station in China. Journal of Environmental Sciences, 26(11), 2451-2458.

Zhang, G., Yao, B., Vollmer, M. K., Montzka, S. A., Mühle, J., Weiss, R. F., O'Doherty, S., Li, Y., Fang, S., Reimann, S., 2017. Ambient mixing ratios of atmospheric halogenated compounds at five background stations in China. Atmos. Environ. 160, 55−69.

Zhang, Q., Streets, D.G., Carmichael, G.R., He, K.B., Huo, H., Kannari, A., Klimont, Z., Park, I.S., Reddy, S., Fu, J.S., Chen, D., Duan, L., Lei, Y., Wang, L.T., Yao, Z.L., 2009. Asian emissions in 2006 for the NASA INTEX-B mission. Atmos. Chem. Phys. 9, 5131–5153.

Zhang, Y.L., Guo, H., Wang, X.M., Simpson, I.J., Barletta, B., Blake, D.R., Meinardi, S., Rowland, F.S., Cheng, H.R., Saunders, S.M., Lam, S.H.M., 2010. Emission patterns and spatiotemporal variations of halocarbons in the Pearl River Delta region, southern China. J. Geophys. Res. 115, D15309.

Zheng, P., Chen, T., Dong, C., Liu, Y., Li, H., Han, G., Sun, J., Wu, L., Gao, X., Wang, X., Qi, Y., Zhang, Q., Wang, W., Xue, L., 2019. Characteristics and sources of halogenated hydrocarbons in the Yellow River Delta region, northern China. Atmos. Res. 225, 70-80.

Zhou, L.X., Tang, J., Wen, Y.P., Li, J., Yan, P., Zhang, X. C., 2003. The impact of local winds and long-range transport on the continuous carbon dioxide record at Mount Waliguan, China. Tellus Ser. B. 55, 145-158.

Table 1. Background and pollution mixing ratios of CH_3CCl_3 at the Shangdianzi Station from October 2006 to December 2017

Year	N[a]) total	Percentage of background	background mixing ratio (ppt)		Pollution mixing ratio (ppt)			
			Mean	S.D. [b]	Mean	S.D.	10%	90%
2006[c]	1198	48%	14.2	10.4	16.1	11.5	14.5	18.6
2007	5503	41%	13.1	10.4	15.1	10.4	13.2	17.7
2008	5122	51%	11.1	8.3	12.5	9.5	10.7	14.1
2009	4619	61%	9.0	5.9	10.0	8.1	8.9	10.8
2010	4548	61%	7.7	5.4	8.5	7.3	7.6	9.1
2011	4590	71%	6.7	4.5	7.1	6.3	6.5	7.6
2012	2761	80%	5.6	4.1	6.0	5.6	5.7	6.3
2013	1943	87%	4.5	3.8	4.8	4.7	4.5	5.1
2014	3492	91%	3.9	2.4	4.2	4.1	3.8	4.4
2015	573	87%	2.8	2.7	3.0	3.0	3.0	3.1
2016	4306	92%	2.7	1.6	2.9	2.9	2.8	3.1
2017	5107	95%	2.4	1.2	2.7	2.6	2.5	2.8

[a]) Number of valid data points.
[b]) Standard deviation (one sigma).
[c]) Observations started in October 2006.

Table 2. Mean and enhancement of CH_3CCl_3 mixing ratios of polluted events at 7 Chinese stations based on monthly/weekly flask samples taken from September 2010 to December 2017.

Year		2010	2011	2012	2013	2014	2015	2016	2017
Lin'an (LAN)	POL/SUM [a])	55%	28%	18%	26%	12%	7%	4%	5%
	No. Pol [b])	6	10	9	11	5	3	2	2
	Mean (ppt)	8.3	7.5	5.7	5.1	4.7	3.7	4.8	2.6
	S.D. (ppt) [c])	1.1	1.6	0.3	0.7	0.4	0.2	2.4	0.3
	ΔAvg (ppt) [d])	1.0	0.9	0.3	0.7	0.9	0.5	2.1	0.3
	ΔMedian (ppt) [e])	0.5	0.5	0.2	0.7	0.9	0.7	2.1	0.4
Longfengshan (LFS)	POL/SUM		9%	13%					
	No. Pol		4	5					
	Mean (ppt)		6.7	5.9					
	S.D. (ppt)		0.9	0.05					
	ΔAvg (ppt)		0.4	0.5					
	ΔMedian (ppt)		0.03	0.5					
Shangdianzi	POL/SUM	33%		8%	5%				2%

(SDZ)	No. Pol	3		3	2				1
	Mean (ppt)	8.0		6.6	5.1				3.0
	S.D. (ppt)	0.6		0.9	0.1				
	ΔAvg (ppt)	0.7		1.1	0.6				0.7
	ΔMedian (ppt)	0.4		0.7	0.6				0.7
Heyuan (HYN)	POL/SUM	-							2%
	No. Pol								5
	Mean (ppt)								2.4
	S.D. (ppt)								0.2
	ΔAvg (ppt)								0.2
	ΔMedian (ppt)								0.2
Jiangjin (JGJ)	POL/SUM	-							8%
	No. Pol								19
	Mean (ppt)								2.8
	S.D. (ppt)								0.5
	ΔAvg (ppt)								0.6
	ΔMedian (ppt)								0.5

[a)] Percentage of data representing polluted conditions.
[b)] Number of samples representing polluted conditions.
[c)] Standard deviation (one sigma)
[d)] △Avg, averaged polluted mixing ratios minus averaged background mixing ratios
[e)] △Median, median of polluted average mixing ratios minus averaged background mixing ratios

Table 3. Emission estimates for CH_3CCl_3 for the North China Plain and the whole of China based on tracer-ratio method and *in-situ* measurement at the Shangdianzi Station. All emissions are given in kt/yr. Uncertainty estimates represent 95% confidence limits.

Year	North China Plain	China
2007	0.8 ± 0.3	1.6 ± 0.6
2008	0.8 ± 0.3	1.5 ± 0.6
2009	0.4 ± 0.2	0.8 ± 0.3
2010	0.4 ± 0.1	0.7 ± 0.3
2011	0.4 ± 0.1	0.7 ± 0.3
2012	0.2 ± 0.1	0.5 ± 0.2
2013	0.2 ± 0.1	0.3 ± 0.1

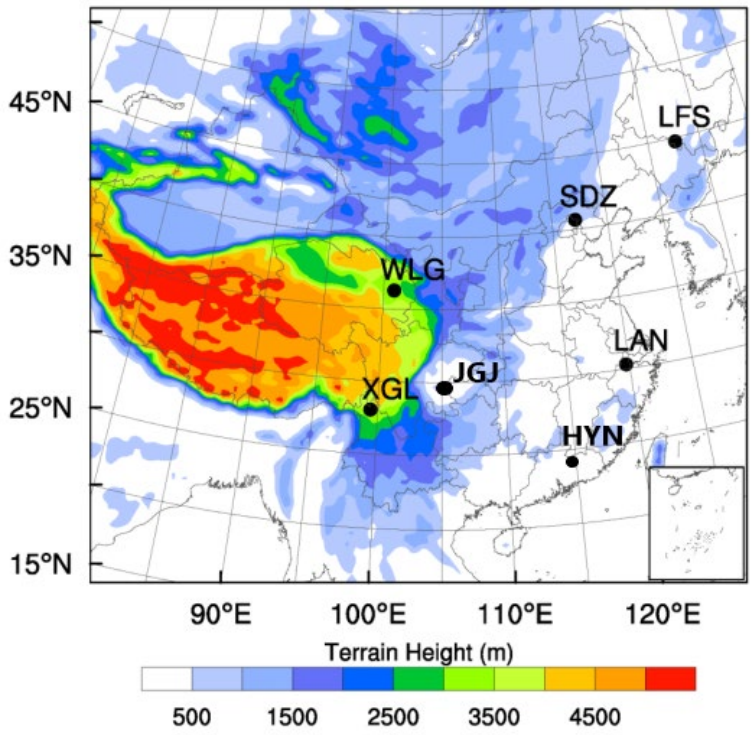

Figure 1. Geographic locations of the sampling stations used in this study. The stations are Shangdianzi (SDZ), Mt. Waliguan (WLG), Shangri-La (XGL), Lin'an (LAN), Heyuan (HYN), Jiangjin (JGJ) and Longfengshan (LFS).

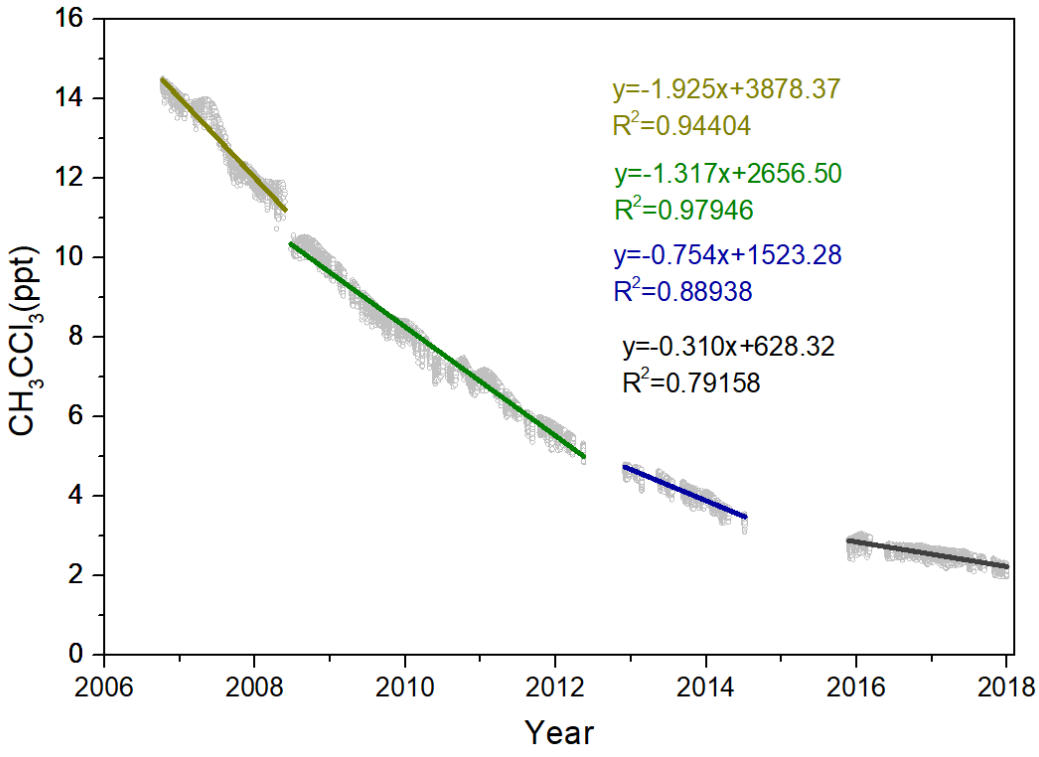

Figure 2. Long-term trends of CH_3CCl_3 mixing ratios at the Shangdianzi Station.

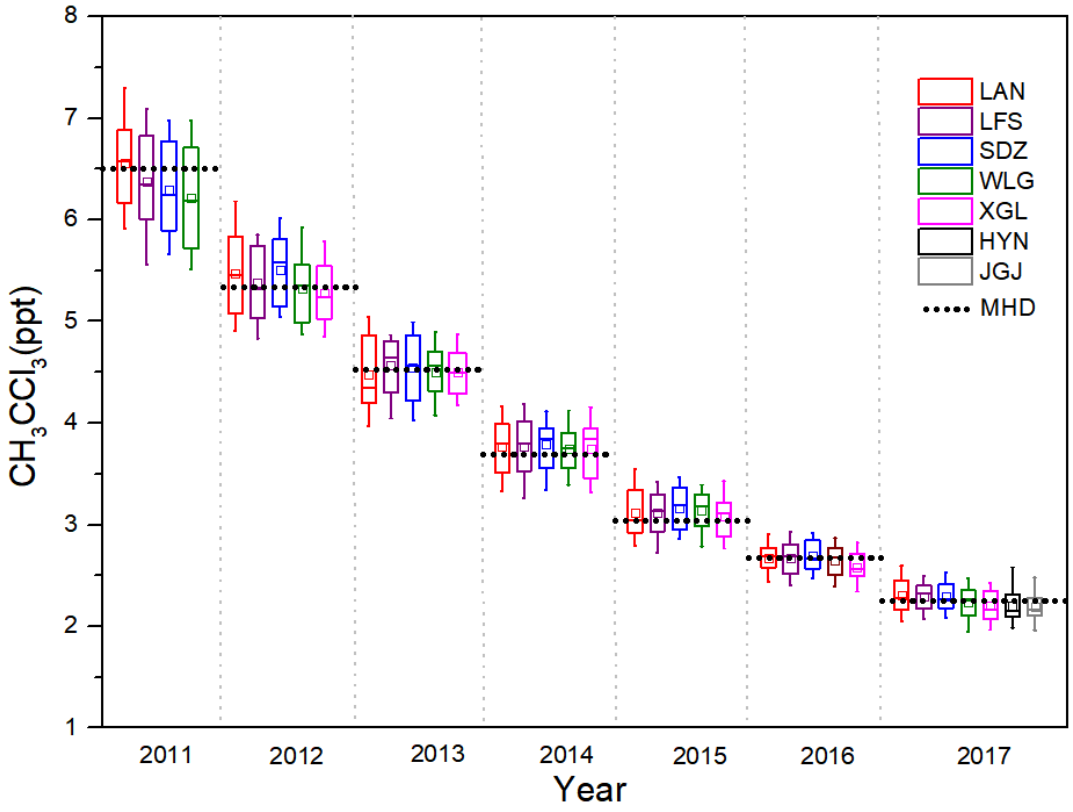

Figure 3. Comparison of background mixing ratios at 7 Chinese Stations and Mace Head, Ireland (MHD) from 2011 to 2017 by GC-MS system. Shown are averages (solid squares), medians (dashes), and 5-, 25-, 75- and 95 percentiles (rectangles). The 7 Chinese stations are Shangdianzi (SDZ), Mt. Waliguan (WLG), Shangri-La (XGL), Lin'an (LAN), Heyuan (HYN), Jiangjin (JGJ) and Longfengshan (LFS).

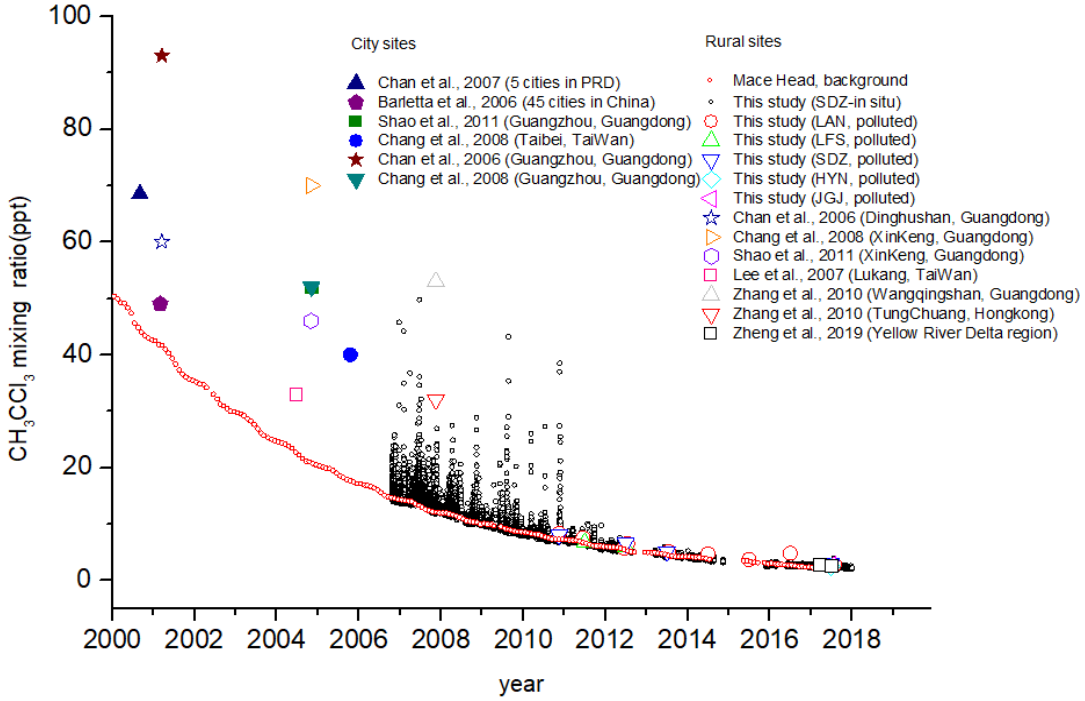

Figure 4. Comparison of CH_3CCl_3 mixing ratios with previous studies in China from 2000 to 2017. SDZ-in situ represents the *in-situ* measurement by GC-ECD system at Shangdianzi, while SDZ, LFS, LAN, HYN, JGJ represent the yearly averaged mixing ratios of pollution events at Shangdianzi, Longfengshan, Lin'an, Heyuan, Jiangjin from this study. Mace Head, background means the average monthly mixing ratio of background conditions at the Mace Head Station by GC-MD system which represent the global background level of northern hemisphere.

Supplementary Material

Atmospheric CH_3CCl_3 observation in China: Historical trends and implications

Dajiang Yu[1], Bo Yao[2,*], Weili Lin[3], Martin K. Vollmer[4], Baozhu Ge[5], Gen Zhang[6], Yi Li[6], Honghui Xu[7], Simon O'Doherty[8], Liqu Chen[2], Stefan Reimann[4]

[1] Longfengshan Regional Background Station, China Meteorological Administration (CMA), Heilongjiang, China

[2] Meteorological Observation Center (MOC) of China Meteorological Administration (CMA), Beijing, China

[3] College of Life and Environmental Sciences, Minzu University of China, Beijing, China

[4] Laboratory for Air Pollution and Environmental Technology (Empa), Swiss Federal Laboratories for Materials Science and Technology, Dübendorf, Switzerland

[5] State Key Laboratory of Atmospheric Boundary Layer Physics and Atmospheric Chemistry, Chinese Academy of Sciences, Institute of Atmospheric Physics, Beijing, China

[6] State Key Laboratory of Severe Weather & Key Laboratory of Atmospheric Chemistry of China Meteorological Administration (CMA), Chinese Academy of Meteorological Sciences (CAMS), Beijing, China

[7] Zhejiang Institute of Meteorological Sciences, Hangzhou, China

[8] Atmospheric Chemistry Research Group, University of Bristol, Bristol, UK

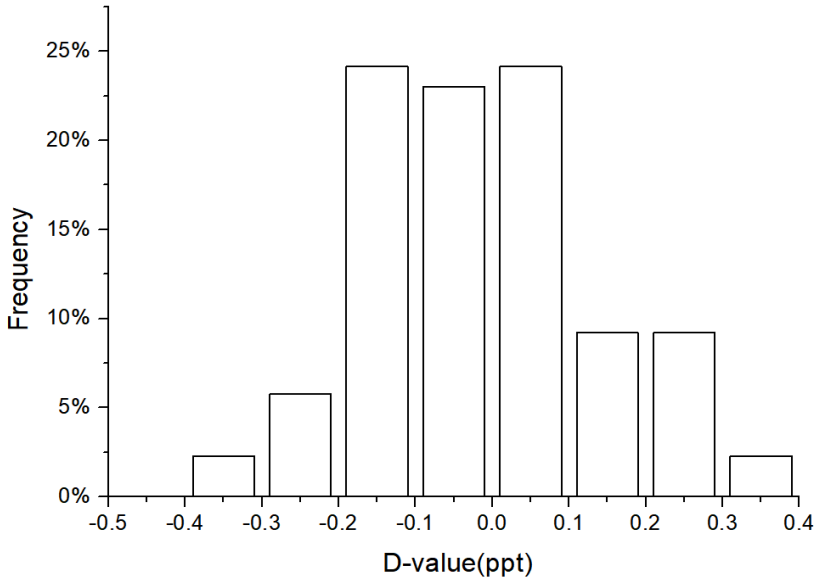

Fig S1. Frequencies of the differences between the mixing ratios of *in-situ* measurement and canister sampling which were taken at most 2 h apart from each other.

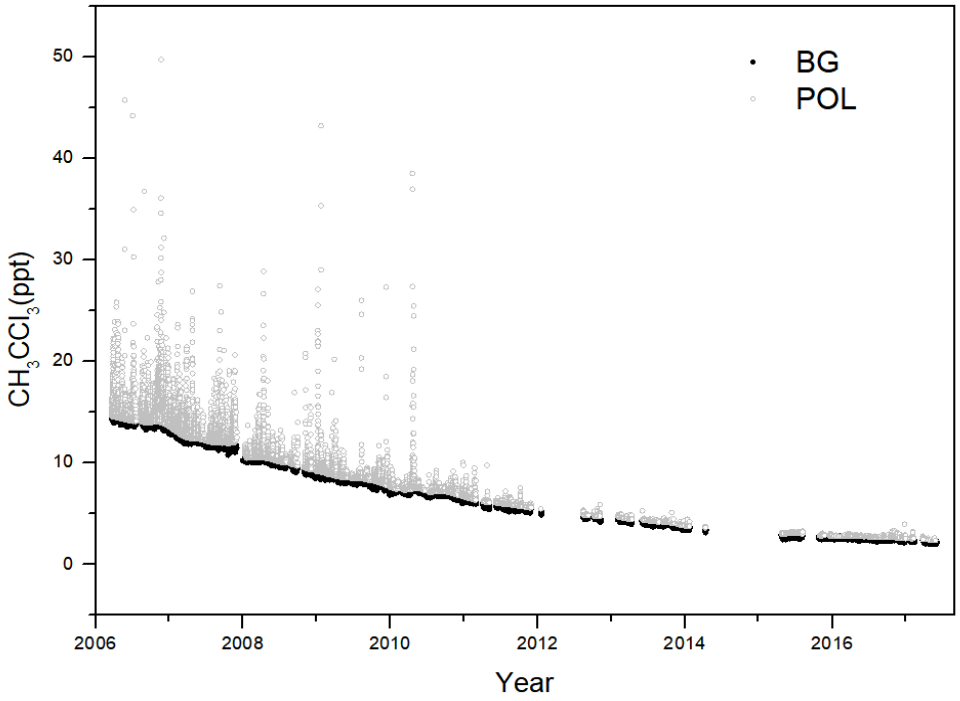

Fig S2. Time series of CH_3CCl_3 mixing ratios based on *in-situ* GC-ECD analysis at the Shangdianzi Station from 2006 to 2017. The black dots represent background data (BG) while the grey dots represent polluted data (POL).

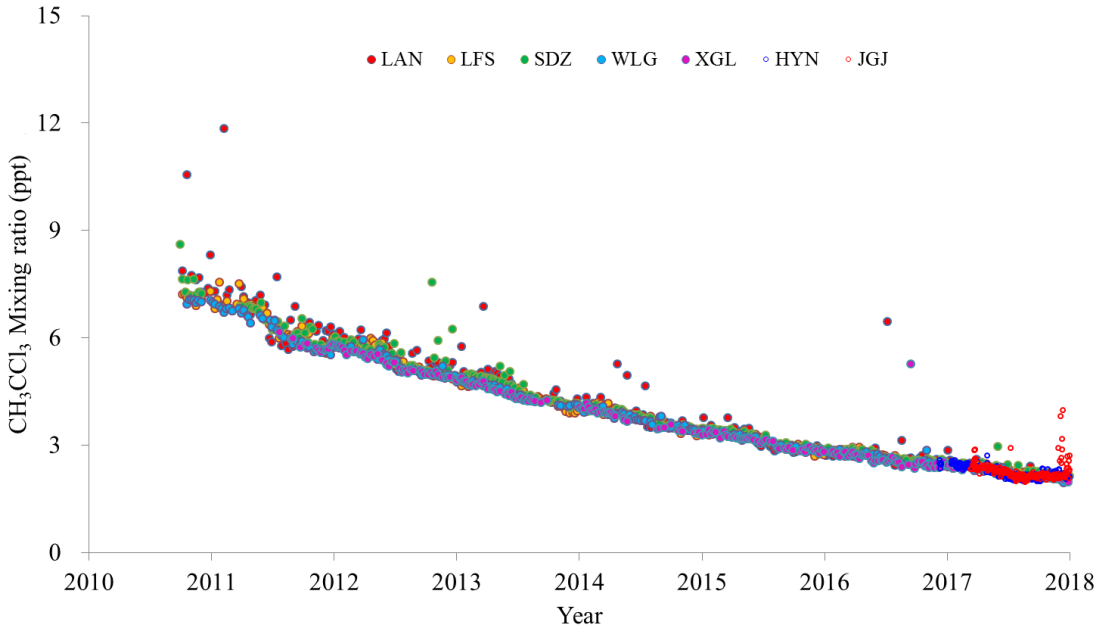

Fig S3. Time series of CH_3CCl_3 mixing ratios of 7 Chinese stations based on weekly/daily sampling and GC-MS analysis from 2010 to 2017. The stations are Shangdianzi (SDZ), Mt. Waliguan (WLG), Shangri-La (XGL), Lin'an (LAN), Heyuan (HYN), Jiangjin (JGJ) and Longfengshan (LFS).

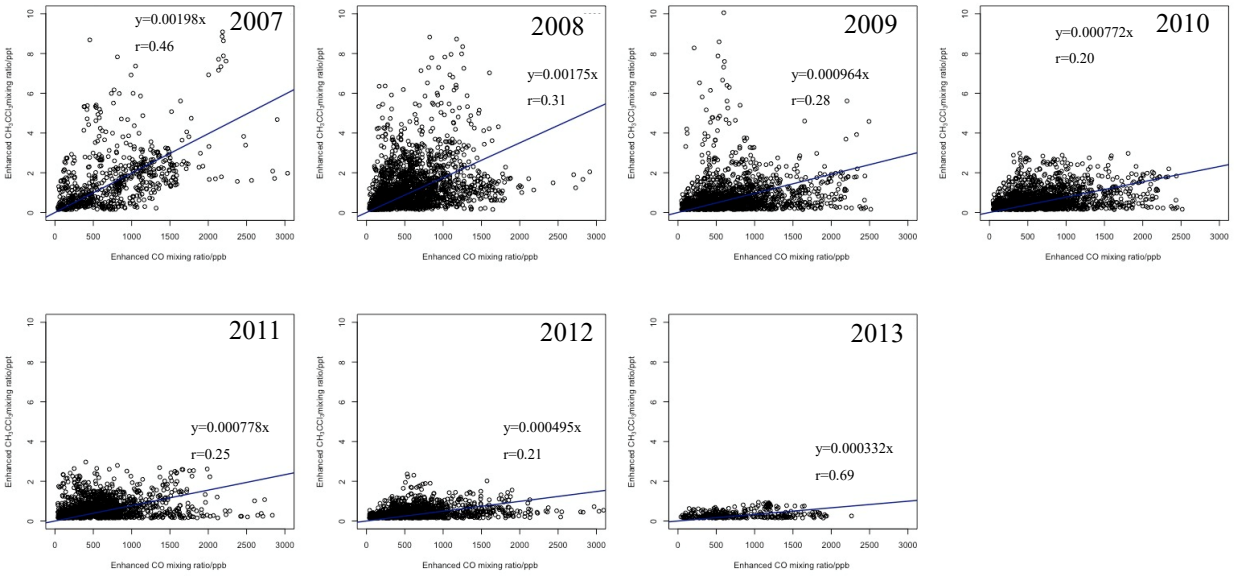

Figure S4: Regression plots of observed enhanced CH_3CCl_3 mixing ratios by GC-ECD system at SDZ versus enhanced CO mixing ratios from 2007 to 2013 (note: the intercepts were set as zero). The results of regression are indicated by the black solid lines.

Table S1. Geographic information, sampling frequency, instrument and observation period of each station

Station	Identifier	Longitude (°E)	Latitude (°N)	Altitude (m)	Measurement since	Sampling frequency	Instrument	Representative
Shangdianzi	SDZ	117.12	40.65	293	October 2006	In-situ/2h	GC-ECD	Northern China Plain
Shangdianzi	SDZ	117.12	40.65	293	September 2010	Weekly	GC/MS	
Mt. Waliguan	WLG	100.90	36.29	3816	October 2010	Weekly	GC/MS	Central Euroasian Continent
Lin'an	LAN	119.73	30.30	138	September 2010	Weekly	GC/MS	Yangtze River Delta
Longfengshan	LFS	127.60	44.73	330	September 2010	Weekly	GC/MS	Northeast China Plain
Shangri-la	XGL	99.44	28.01	3580	July 2011	Weekly	GC/MS	Yunnan-Guizhou Plateau
Heyuan	HYN	114.60	23.69	1076	January 2017	Daily	GC/MS	Pearl River Delta
Jiangjin	JGJ	106.15	29.15	262	March 2017	Daily	GC/MS	Sichuan Basin